Relationship of magnetic ordering and crystal structure in the lanthanide ferromagnets Gd, Tb, Dy, and Ho at high pressures

Masaki Mito,[1,*] Yuta Kimura,[1] Kanako Yamakata,[1] Masahiro Ohkuma,[1] Hirotaka Chayamichi ⦿,[1]
Takayuki Tajiri,[2] Hiroyuki Deguchi,[1] and Mamoru Ishizuka[3]

[1]*Graduate School of Engineering, Kyushu Institute of Technology, Kitakyushu 804-8550, Japan*
[2]*Faculty of Science, Fukuoka University, Fukuoka 814-0180, Japan*
[3]*Center for Scientific Instrument Renovation and Manufacturing Support, Osaka University, Toyonaka 560-8531, Japan*

The pressure dependence of the magnetic ordering temperatures for the lanthanide ferromagnets Gd, Tb, Dy, and Ho has been investigated in the pressure region up to 18 GPa by two types of magnetic measurements using a superconducting quantum interference device (SQUID). The present magnetic measurements enabled us to investigate the pressure dependence of the magnetization intensity at low magnetic fields as well as the magnetic ordering temperatures. Their results are interpreted in the light of such previous experiments as magnetic susceptibility, magnetization, electrical resistance, neutron diffraction, and Mössbauer spectroscopy measurements. All of the magnetic orderings in the above four elements were suppressed down to less than the detection level, being related to the structural transition. The ferromagnetic ordering in Gd, Tb, Dy, and Ho is stabilized in the hcp structure. The magnetic anomalies due to the helimagnetic ordering of Tb and Dy disappear at the Sm-to-dhcp transition and the hcp-to-Sm transition, respectively, while that of Ho disappears in the Sm-type phase near the Sm-to-dhcp transition.

I. INTRODUCTION

Ferromagnetic metals have been important subjects in condensed matter physics from the viewpoint of magnetism originating from itinerant electrons. In the $4f$ lanthanide series, there are six ferromagnetic (FM) elements Gd, Tb, Dy, Ho, Er, and Tm. The ferromagnetism is explained by the RKKY interaction among localized moments of the f-orbital electrons mediated by the conduction electrons [1–3]. The spatially damped oscillation of the conduction electron spin polarization is indicative of the competition between the FM and antiferromagnetic correlations, which often results in an incommensurate antiferromagnetic structure, e.g., the helimagnetic (HM) structure. Hereafter the magnetic transition temperatures between the FM and HM states and the transition temperatures between the HM and paramagnetic states are denoted as T_C and T_N, respectively.

The aforementioned ferromagnetism is modified when the crystal structure changes. All $4f$ lanthanide ferromagnets, Gd–Tm, have an hcp structure at ambient pressure, and exhibit the structural transformations hcp → Sm-type → double-hcp (dhcp) → fcc → trigonal under pressure, as shown in Fig. 1 [4,5]. In the periodic table, the antiferromagnet Sm is located two elements to the left of Gd [6]. The variation of the magnetic properties with the structural transformations in $4f$ ferromagnetic metals has been reported by magnetic measurements [7–10], electrical resistance ones [11–16], neutron diffraction [17,18], and Mössbauer spectroscopy [19]. The magnetic measurement mainly detects the sum of the mag-

netic moments of the localized $4f$ electrons, and the electrical measurement detects the transport properties of conduction electrons correlated with localized $4f$ electrons. The electrical measurement has been successful at much higher pressures than the pressure range of the magnetic measurements. The previous magnetic measurements on Gd–Ho under pressure are reviewed below after describing the methods of high-pressure magnetic measurements using a diamond anvil cell (DAC).

There are four methods for magnetic measurements over a wide T range using a DAC: (1) the electromagnetic induction-type AC method using a high-frequency AC field, for instance, Ref. [9]; (2) DC and (3) AC methods using a commercial superconducting quantum interference device (SQUID) magnetometer and a miniature DAC [20]; and (4) vibrating-coil magnetometer (VCM) methods using a SQUID [21]. In general, the measurement sensitivity of magnetization in methods (2)–(4) using a SQUID is better than that of magnetic susceptibility in (1). The accuracy of detecting minute signals (10^{-8} emu) in the AC magnetization (M_{AC}) measurements for (3) is better than that for the DC magnetization (M_{DC}) in (2). Placing a detection coil near a sample and using the lock-in technique in (4) realizes the best accuracy (10^{-9} to 10^{-10} emu) among the aforementioned methods. The experiments by Iwamoto *et al.* [8] and Mito *et al.* [10] used method (2), and those by McWhan and Stevens [7] and by Jackson *et al.* [9] used method (1).

The history of magnetic measurements on $4f$ ferromagnetic metals started with the first measurement by McWhan and Stevens in 1965 [7]. In the experiment, the ring-type Gd–Ho samples were surrounded by both induction and detection coils, and the high-temperature magnetic transitions
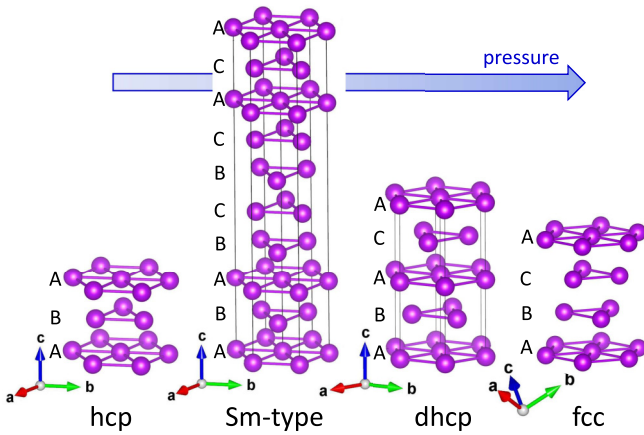
*mitoh@mns.kyutech.ac.jp

FIG. 1. Structural transformation in $4f$ lanthanide ferromagnets Gd–Tm under pressure from hcp $\rightarrow$ Sm-type $\rightarrow$ double-hcp (dhcp) $\rightarrow$ fcc structure. The change in the stacking of hexagonal planes is expressed by naming their planes the A, B, and C planes.

(T_C for Gd; T_N for Tb, Dy, and Ho) were observed through the electromagnetic induction voltage, which corresponds to the AC susceptibility (χ_{AC}) as a function of the temperature T. They observed a decrease in T_C and T_N at high pressures. Indeed, there was a problem that residual strain brings about a complicated T dependence of χ_{AC} at zero DC magnetic field (H_{DC}).

In 2003, Iwamoto *et al.* observed M_{DC} for small pieces of Gd at $H_{DC} = 0.5$ T, enough to increase M_{DC} up to more than 60% of saturated magnetization at ambient pressure, under pressures of up to 8 GPa using method (2) [8]. They observed the reduction in T_C. Subsequently, similar M_{DC} experiments $H_{DC} = 0.3$ or 0.5 T were also performed on Tb, Dy, and Ho under pressures of up to 9 GPa by the same group [10]. H_{DC} of the 0.3–0.5 T level is enough to assume the change in the magnitude of the saturated magnetization as a function of pressure. The pressure dependencies of M_{DC} at sufficient H_{DC} as well as both T_C and T_N were investigated, so that the critical pressure P_c values for the disappearance of FM magnetization were estimated as shown in Table I. Furthermore,

the behaviors as their volumes shrunk were also discussed. P_c resulted in a volume shrinkage of approximately 17% for each ferromagnet.

In 2005, Jackson *et al.* measured χ_{AC} in six elements Gd–Tm using magnetoelectric induction methods at AC field of 3 Oe and 10 kHz [9]. They used a microsensing coil positioned on the culet of a diamond anvil, and observed the change in T_C for Gd and Tb and in T_N for Dy and Ho.

The structural phase transitions bring about changes in the spatial distribution of the electron orbital wave function for the electrons, resulting in changes in their electronic structure and/or valence. Indeed, at ambient pressure, the electrical resistance R exhibits a characteristic anomaly at T_C or T_N. Thus, R has been used as a sensitive tool for the pursuit of magnetic ordering based on the assumption that changes in R would reflect magnetic ordering even at high pressures [11–16]. Two groups have conducted the R measurements so far. In their previous high-pressure experiments on Gd, Tb, and Dy except for one study for Tb [12], broad anomalies in R were characterized as magnetic orders even at pressures higher than P_c evaluated by their magnetic measurements [11,13–16]. Although various magnetic factors based on the RKKY as well as the change in electronic structure are reflected in R, it is not reasonable to infer a change in T_C or T_N only from the change in R, especially at high pressures. In fact, for materials with both T_C and T_N, both critical temperatures cannot be determined solely from R even at ambient pressure. Recently, neutron diffraction experiments for Tb [12], Dy [17], and Ho [18] have been reported because of an increasing interest concerning the magnetic ordering at high pressures. In Dy and Ho, peaks originating from the magnetic origin were observed at pressures above P_c determined by previous magnetic measurements [9,10]. Furthermore, for Dy, the synchrotron Mössbauer spectroscopy and x-ray absorption near edge structure have been conducted to study the existence of magnetic order and the change in valence at pressures more than 100 GPa [19].

Thus, the magnetic phase diagram based on R-T measurements and neutron diffraction experiments should be validated against the results of current magnetic measurements. The previously reported results for M_{DC} [8,10], χ_{AC} [9], and R

TABLE I. Critical pressure P_c for the disappearance of ferromagnetic (FM) and helimagnetic (HM) signals in the lanthanide ferromagnetic metals Gd, Tb, Dy, and Ho. Gd has no HM order. NE stands for "not evaluated". In the M_{DC} measurements (by Iwamoto and Mito *et al.* [8,10]), P_c can be estimated at an accuracy of 0.1 GPa based on the pressure dependence of M_{DC} at $H_{DC} = 0.3$ or 0.5 T. In the χ_{AC} measurement (by Jackson *et al.* [9]) and M_{AC} measurement (the present study), the accuracy of P_c depends on the number of measurements as a function of T around P_c. It is on the order of 1 GPa. For reference, there are also reports (by Thomas *et al.* [12], Samudrala *et al.* [11,13], and Lim *et al.* [14–16]) that the R anomaly reflects the FM or HM order. The R anomaly often survives even at high pressures of more than P_c evaluated in the magnetic measurements [11,13–16]. The pressure P'_c at which the anomaly temperature switches from decreasing with increasing pressure to increasing with increasing pressure is also presented.

Element	P_c from M_{DC}	P_c from χ_{AC}	P_c from R	P_c from M_{AC} and M_{VCM}
	[8,10]	[9]	[11–16]	Present study
	FM/HM	FM/HM	FM/HM	FM/HM
Gd	9.0 GPa/–	7 GPa/–	No P_c (P'_c = 18 GPa [11,14,16])/–	6.4 ± 0.3 GPa/–
Tb	7.5 GPa/NE	6–8 GPa/NE	3.6 GPa [12], No P_c (P'_c = 13 GPa [15,16])/NE	7 GPa/17 GPa
Dy	7.6 GPa/NE	4 GPa/8 GPa	NE/No P_c (P'_c = 17 GPa [13], 21 GPa [14,16])	7 GPa/8 GPa
Ho	11.0 GPa/NE	NE/9–12 GPa	Has not been measured	9 GPa/12–16 GPa

[11–16] are summarized in Table I. In the present study, we utilized methods (3) and (4) detecting the magnetization intensity by the lock-in technique to investigate the pressure dependence of the magnetization intensity at low magnetic fields as well as the magnetic ordering temperatures for Gd–Ho at pressures to obtain the pressure-dependent phase diagram and determine P_c for the disappearance of both the FM and HM magnetization down to less than the detection level. The magnetic measurements will then be compared with the results for the R measurements and neutron diffraction measurements in the literature. Finally, we will discuss the relationship between FM and/or HM states and crystal structure via the pressure experiments.

II. METHODS

Polycrystalline samples of Gd, Tb, Dy, and Ho metals with high purity (99.9%) were purchased from Nippon Yttrium Co., Ltd. Some fragments of volume $< 0.1 \times 0.1 \times 0.1$ mm^3 were used in the high-pressure experiments.

The M_{AC} in method (3) was measured using a SQUID magnetometer equipped with an AC option [22–30] at pressures of GPa level, to properly distinguish magnetic anomalies existing over a wide temperature range from background. The main frequency and amplitude of the AC field (H_{AC}) were 10 Hz and 3.9 Oe, respectively. The M_{AC} was divided into the in-phase M'_{AC} and the out-of-phase M''_{AC} components by Fourier transformation. Most of the metallic background contributions appear in M''_{AC}, while the magnetic signal of the targeted materials mainly appears in M'_{AC}. The information of background contributions surviving in M'_{AC} as a function of temperature in the experiments for Gd, Tb, and Ho is presented in the Supplemental Material [31]. As for Dy, the corresponding information will appear in the paper.

Contraction corresponding to a stress of up to 18 GPa was achieved using a miniature CuBe DAC that consisted of two diamond anvils with 0.5 mm diameter flat tips and a 0.25 mm thick Re gasket [20,32]. A liquid-like pressure-transmitting medium (PTM), Apiezon-J oil (Ap-J), was confined together with small pieces of lanthanide metals in the sample chamber. The pressure value at room temperature was evaluated by measuring the fluorescence of ruby [33] located in the sample cavity with the lanthanide metals, and it was evaluated as the pressure value of its measurement (P).

For Ho, a position-sensitive magnetization M_{VCM} was also measured using a vibrating-coil SQUID magnetometer [method (4)] [21,34,35] to confirm the origin of the M'_{AC} anomaly similar to the superconducting signal. Then, a NiCrAl-CuBe composite gasket was used [36]. The small fragments were placed in the sample cavity together with the PTM, Daphne oil 7373, ruby, and lead. The ruby served as a room-temperature manometer, and the lead as a manometer at the liquid-^{4}He temperature. M_{VCM} at H_{DC} of 2.0 Oe was then observed during the warming process after zero-field cooling.

III. EXPERIMENTAL RESULTS

A. Gd

Figure 2 shows the T dependence of the M'_{AC} for Gd [the first and second runs were at $H_{DC} = 0$ (a) and the third run was
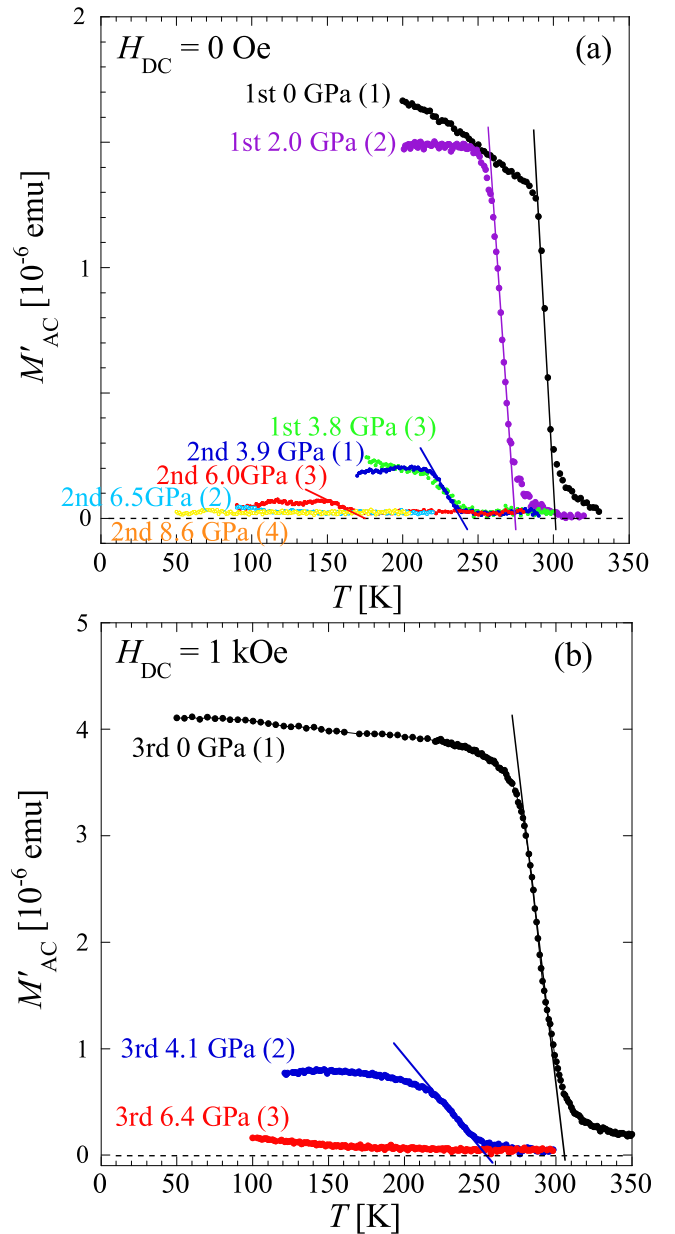

FIG. 2. T dependence of M'_{AC} for Gd at $H_{DC} = 0$ (a) and 1 kOe (b), measured by method (3). The number in parentheses gives the order of the measurement number for each run.

at $H_{DC} = 1$ kOe (b)]. As seen in (a), at $P = 0$, M'_{AC} increases with decreasing temperature below 300 K. The FM anomaly shifts toward the low-T side at $P = 2.0$ GPa, almost keeping the magnitude of M'_{AC}. Compared to the magnitudes of M'_{AC} in the hcp phase for $P = 0$ and 2.0 GPa, the magnitudes in the Sm-type phase (2 GPa $< P <$ 6 GPa) are reduced to less than one-fifth of the former. In the dhcp phase ($P >$ 6 GPa), the intensity of M'_{AC} drops to the noise level. The aforementioned behavior was also confirmed in the M'_{AC} measured at $H_{DC} = 1$ kOe [see (b)]. Thus, when the hcp-to-Sm phase transition occurs, M'_{AC} begins to decrease. According to a previous work on XRD analysis [10], the XRD profile for 2 GPa $< P <$ 6 GPa is reproduced with the sum of the hcp and Sm-type phases. The intensity of M'_{AC} reflects the summation of the
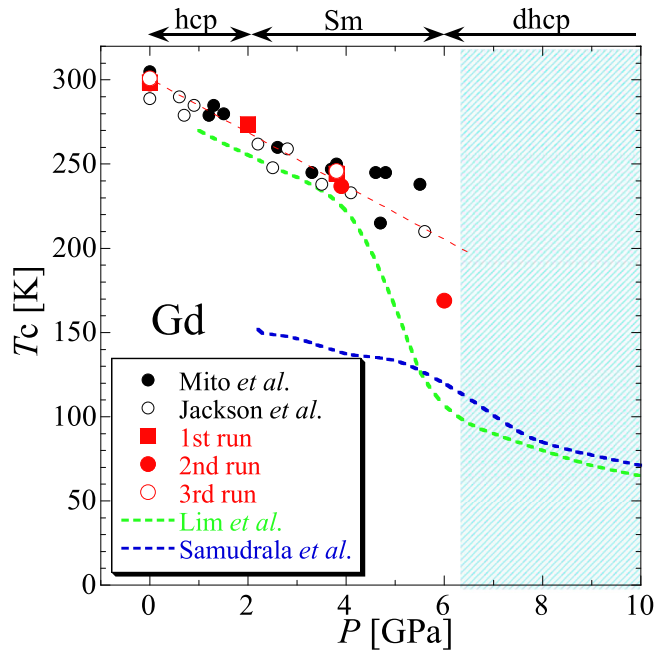
FIG. 3. P dependence of T_C for Gd. The data in the literature on magnetic measurements such as by Mito *et al.* [8,10] and Jackson *et al.* [9] and on electrical measurements by Samudrala *et al.* [11] and Lim *et al.* [14,16] are also presented.

FIG. 4. T dependence of M'_{AC} for Tb at $H_{DC} = 0$, measured by method (3). The T_N (high-T side) and T_C (low-T side) are marked with arrows, and their changes are traced with lines.

magnetic moments of magnetic domains. There, the volume of surviving hcp domains decreases with increasing pressure, resulting in a decrease in M'_{AC}. Afterward, when the Sm-to-dhcp phase transition occurs, the M'_{AC} characteristic of FM order disappears. The results suggest that the FM state of Gd intrinsically originates from the hcp phase. This assumption will be supported by the results of R by Samudrala *et al.* [11], which show the discrete change in T_C at the hcp-to-Sm phase transition. T_C was evaluated from the intersection between the solid line with the largest gradient and the dashed baseline [see Figs. 2(a) and 2(b)]. The T_C evaluated at $P = 0$ was estimated to be approximately 300 K, which is consistent with the values reported in the literature [7–10].

Figure 3 shows the P dependence of T_C in Gd, together with the data from previous magnetic [8–10] and R measurements [11,14,16]. The R anomaly observed by Lim *et al.* demonstrates almost consistent behavior with T_C evaluated via a series of magnetic measurements for $P < 4$ GPa. In all the magnetic measurements by both Jackson *et al.* and us, T_C could not be determined for $P > 6$ GPa, because of the minute magnetic signal below the noise level. The disappearance of the FM signal can be reasonably related to the structural transition from the Sm-type phase including the surviving hcp domains to dhcp structures. The T_C determined from the R anomaly traces the change in T_C evaluated from the magnetic measurements for 2–4 GPa. There are also data for T_C determined from R below 100 K even in the dhcp phase. The R results by Samudrala *et al.* exhibit large deviations from the data by Lim *et al.* for $P < 5$ GPa, where they also observed the minimum T_C at approximately 18 GPa [11].
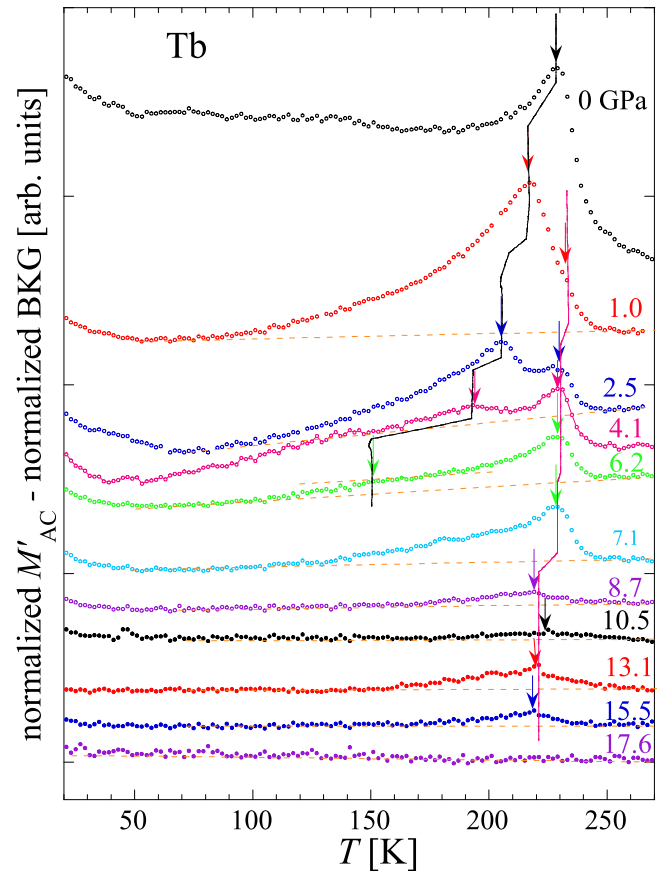
B. Tb

Figure 4 shows the T dependence of M'_{AC} in Tb at $H_{DC} = 0$. Herein, the background signal normalized by the signal at the highest T is subtracted from M'_{AC} normalized by the value at the highest T. There is a cusp at 230 K at $P = 0$, where anomalies in both T_N and T_C exist within a narrow temperature range, and the determination of each separately is difficult. At $P = 1.0$ GPa, a small shoulder due to the HM order appears on the high-T side of the cusp anomaly due to the FM order, and the determination of T_N and T_C becomes possible. With increasing P, the FM anomaly shifts further toward the lower-T side, with a decreased magnetic intensity. The determination of T_C is possible up to $P = 6.2$ GPa with proper subtraction of the background. Within the hcp phase (< 5 GPa), the FM anomaly exists as a prominent M'_{AC} anomaly. After transforming to the Sm-type phase, the FM order becomes unstable. On the other hand, the shoulder due to the HM order, pointed out at $P = 1.0$ GPa, becomes sharp because the FM anomaly is far away from the HM order, and it exists prominently at approximately 230 K up to $P = 7.1$ GPa. For 8.7–15.5 GPa, the HM order survives as a small anomaly around 220 K. Boundaries exist between 7.1 and 8.7 GPa for both the T_N value and the anomaly intensity. At $P = 17.6$ GPa, the HM anomaly cannot be observed. The above critical pressure is slightly lower than pressure for the structural phase transition from the Sm-type to dhcp structures. Indeed, this HM order at 4.9 GPa was also
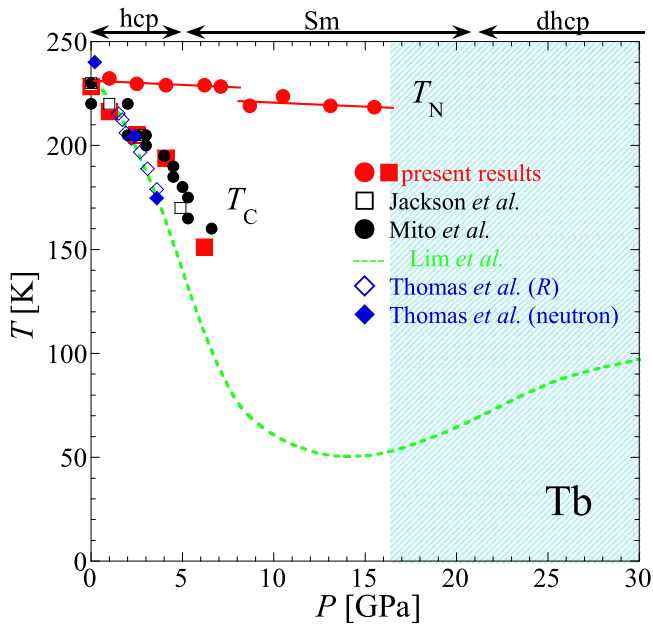
FIG. 5. P dependence of T_N and T_C for Tb. The data in the literature on magnetic measurements by Mito *et al.* [10] and Jackson *et al.* [9], electrical resistance (R) measurements by Thomas *et al.* [12] and Lim *et al.* [15,16], and neutron diffraction [12] are also presented.

observed as a broad hump in electromagnetic induction AC measurements under an AC field of 10 kHz by Jackson *et al.* [9].

Figure 5 shows the P dependence of T_N and T_C in Tb, together with the data from previous magnetic measurements [8–10] and R measurements [12,15,16]. For the P dependence of T_C, there is reasonable consistency among the present results, the results from the previous magnetic measurements by both us [8,10] and Jackson *et al.* [9], and the T_C evaluated from the R measurements by Thomas *et al.* [12] and Lim *et al.* [15,16]. This suggests that the R anomaly in Tb reflects the FM order, because T_N hardly changes for $P \leqslant 7.1$ GPa.

The results of R by Thomas *et al.* exhibit the disappearance of the FM anomaly near the phase boundary between the hcp and Sm-type phases [12], consistently with the present magnetic data. The neutron diffraction due to the FM order exhibits behavior similar to R [12]. The R anomaly observed by Lim *et al.*, however, suggests the survival of FM order even for $P \geqslant 6.2$ GPa, and the results by Lim *et al.* might reflect deviations from three-dimensional magnetic ordering. Indeed, at high P, the R anomaly tends to show broad changes over a wide T range. In Tb, we want to keep the possibility that the R measurement results reflect arbitrary characteristic changes that are possible for the conduction electrons within the temperature region, where the RKKY interaction becomes dominant over the thermal fluctuation.

C. Dy

Figure 6 shows the T dependence of M'_{AC} in Dy at $H_{DC} = 0$ over two runs. The first run is shown in (a), and the second run is shown in (b). Two magnetic anomalies of the HM and FM orders appear over a wide T range. Therefore, the
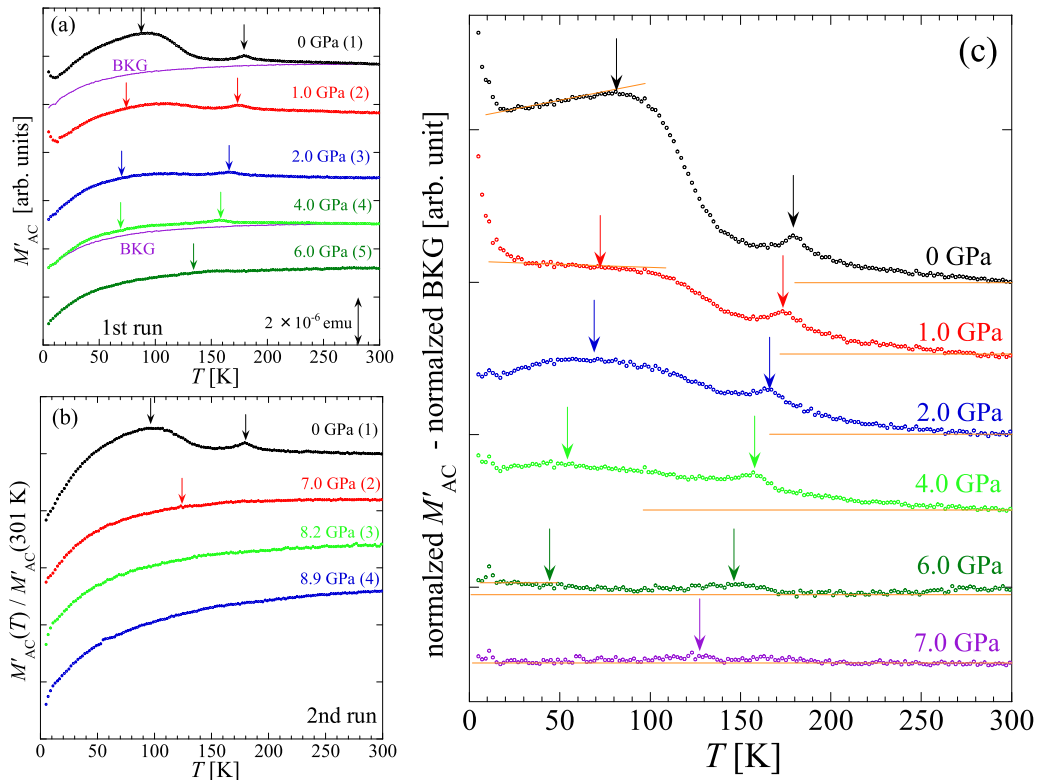

FIG. 6. T dependence of M'_{AC} in Dy at $H_{DC} = 0$. T_N (high-T side) and T_C (low-T side) are marked with arrows, and their changes are traced with lines. (a) M'_{AC} in the first run, (b) M'_{AC} in the second run, and (c) normalized M'_{AC} after subtracting the normalized background contribution. In (a) and (b), the number in parentheses gives the order of the measurement number for each run.
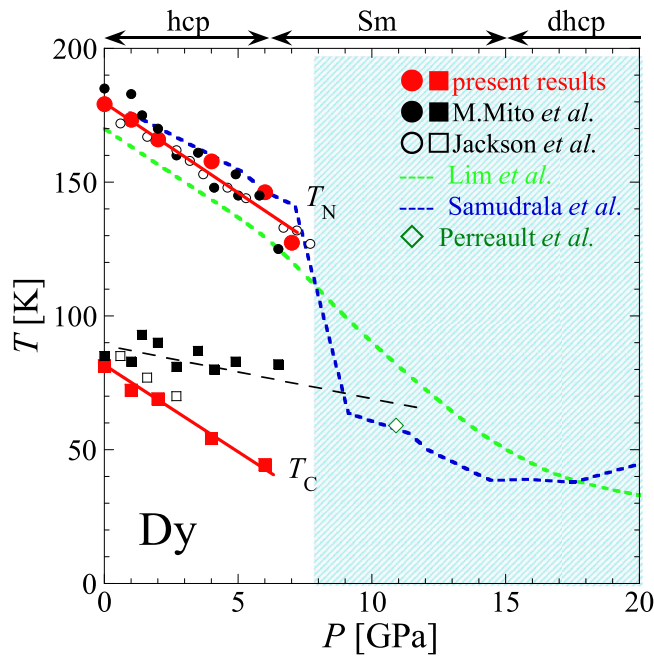
FIG. 7. *P* dependence of T_N and T_C for Dy. The data in the literature on magnetic measurements by Mito *et al.* [10] and Jackson *et al.* [9] and on electrical measurements by Samudrala *et al.* [13] and Lim *et al.* [15,16] are also presented. Referring to Fig. 6(c), the anomalies determined by Lim *et al.* appear at around the positions of the minimum M'_{AC} between T_N and T_C. The transition temperature determined from R by Samudrala *et al.* [13] follows T_N determined in the present data and, for $P > 7$ GPa, it approaches the broken extrapolated line of T_C evaluated from the M_{DC} data at $H_{DC} = 0.3$ T by Mito *et al.* [10]. For reference, in the neutron diffraction experiment by Perreault *et al.* [18], the temperature at which the nuclear peak with a magnetic origin appears is also marked. It is also on the extrapolated line of T_C evaluated from the M_{DC} data by Mito *et al.* [10].

background contributions in (a) and (b) have not been deleted so that the magnetic anomalies can be studied. At $P = 0$, the HM anomaly appears as a small cusp at approximately 180 K, and the FM anomaly appears as a broad hump at approximately 90 K. The effect of pressure on the intensity of the FM anomaly is more prominent than that on the HM anomaly. The FM anomaly vanished at $P = 6.0$ GPa, whereas the HM anomaly was observed until $P = 7.0$ GPa. The data after subtracting the background contribution are shown in Fig. 6(c). Figure 6(c) reveals that the two anomalies shift toward the lower-T side at higher pressures while maintaining an almost constant T separation.

Figure 7 shows the P dependence of both T_N and T_C in Dy, together with the data from previous magnetic [9,10] and R measurements [13,14,16]. For the decrease in T_N with increasing P, there is good consistency between the results of the present magnetic measurements and those by Jackson *et al.* The results of R by Samudrala *et al.* show rapid decrease in T_N at the phase boundary between the hcp and Sm-type phases [13], and it is consistent with the suppression of the HM magnetization down to less than the detection level in the present experiments. In both results by Samudrala *et al.* [13] and Lim *et al.* [14,16], the R anomaly after the hcp-to-Sm structural transition appears on the extrapolated line

of T_C determined by M_{DC} at $H_{DC} = 0.3$ T [10]. For T_C, the present SQUID-based AC measurement [method (3)] reveals an observation that T_C decreases in a parallel manner to T_N. With method (3), T_C could be determined until just after the transformation to the Sm phase. The FM anomaly of M'_{AC} is quite broad. Therefore, it might be difficult to detect the FM anomaly by the M_{DC} measurement [method (2)] at high H_{DC} and the χ_{AC} measurement [method (1)] with a high-frequency AC field. Indeed, even with method (3), there is ambiguity in determining T_C.

In contrast to Tb, both T_N and T_C in Dy decrease with increasing P. Considering the behavior in the hcp phase to simplify the discussion, the appearance of the R anomaly in Tb traces the change in T_C, whereas that of the R anomaly in Dy does the change in T_N. The series of results for Tb and Dy suggests that the physics reflected in R depends on the metals.

D. Ho

Figures 8 and 9 show the T dependence of M'_{AC} in Ho measured over three runs (Fig. 8: the first run, Fig. 9: the second and third runs). At $P = 0$, the HM order appears at approximately 130 K, and the FM order at 18 K. In the previous M_{DC} measurements at high H_{DC}, the magnetic anomaly of the HM order at $P = 0$ appeared prominently, whereas the HM anomaly in the present M_{AC} at $H_{DC} = 0$ is small. As shown in Fig. 8(a), the HM anomaly in M'_{AC} grows with increasing P and shifts toward the lower-T side. It survives even after the crystal structure has transformed into the Sm-type structure. However, the intensity of the FM anomaly decreases with increasing P, and the anomaly cannot be detected just above the critical pressure for the transition from the hcp to the Sm-type structures. Figure 8(a) presents the experimental data measured as P was first increased to 11.2 GPa. After P has reached 11.2 GPa, it was reduced to 0.5 GPa [see Fig. 8(b)], and then increased to 11.6 GPa. Figure 8(b) presents the data measured as P was increased from 0.5 to 11.6 GPa for the second time. The inset shows the M'_{AC} at H_{AC} of both 3 and 10 Hz and some values of H_{DC}. The FM anomaly at $P = 0.5$ GPa was reduced to approximately 30% of the initial one. Furthermore, even at the following $P = 11.6$ GPa, FM anomalies were observed. This suggests that the residual strain disturbs the disappearance of the FM order. Thus, the disappearance of the FM magnetization is related to the structural phase transition. Furthermore, the FM anomaly at $P \neq 0$ resembles the superconducting signal. For instance, at $P = 10.1$ GPa, the behavior does not depend on whether the frequency of H_{AC} was 3 or 10 Hz, as can be seen from the inset of Fig. 8(b). Because the anomalies observed at $P = 10.1$ GPa disappear at H_{DC} on the order of 100 Oe and do not shift toward the lower-T side, we can dismiss the possibility of superconductivity here.

The behaviors for both the HM and FM orders were also observed in the second run, as shown in Fig. 9(a). The FM anomaly changes to a superconducting-like signal at 6.9–7.2 GPa. It was confirmed again that the superconducting-like signal was suppressed by H_{DC} on the order of 40 Oe, as shown in the inset of Fig. 9(a). This behavior of the FM order suggests that the thermal stability of the FM domain formation
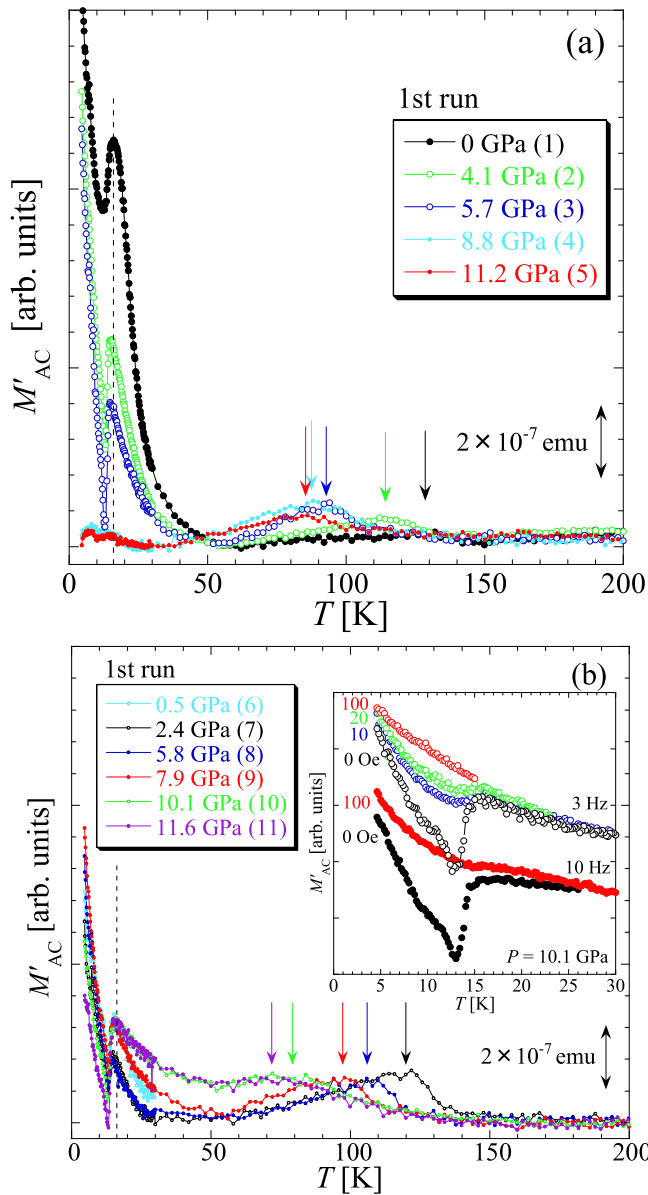
FIG. 8. T dependence of M'_{AC} in the first run for Ho at $H_{DC} = 0$, measured by method (3). T_N (at high-T side) is marked with an arrow, and T_C (at low-T side) at $P = 0$ is marked with a dotted line. The number in parentheses gives the order of the measurement number. The data for sequences of (1)–(5) and (6)–(11) are shown in (a) and (b), respectively.

does not vary for $P < P_c$, whereas the size of the FM domain is reduced with increasing P. On the other hand, as shown in Fig. 8(a), the HM order can survive even after the FM anomaly disappears. Indeed, at $P = 16.0$ GPa, the HM order also disappears, as shown in Fig. 9(b).

As mentioned above, M_{DC} at sufficient H_{DC} is unsuitable for the determination of T_C. In order to confirm whether the signal at around 15 K is a superconducting signal or not, we measured the magnetization at small H_{DC} for $P \leqslant 12.7$ GPa using the SQUID VCM method [method (4)], as shown in Fig. 10; panel (a) shows the first run for $P \leqslant 8.2$ GPa and (b) the second run for $P = 0$ and 12.7 GPa. The measured
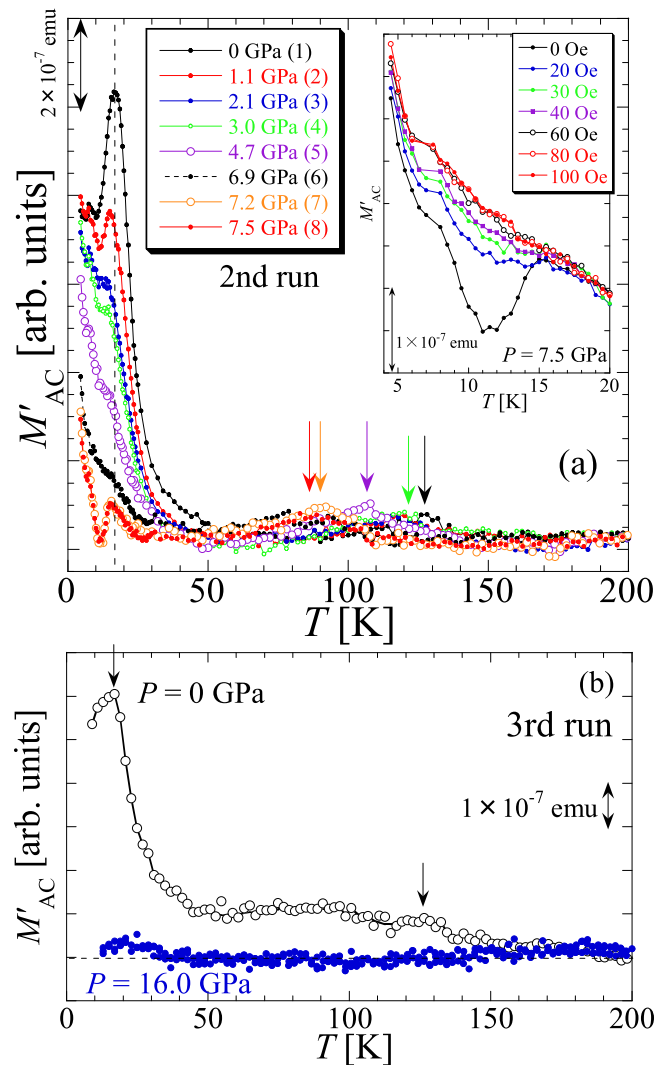

FIG. 9. T dependence of M'_{AC} in the second (a) and third (b) runs for Ho at $H_{DC} = 0$, measured by method (3). In (a), T_N (at high-T side) is marked with an arrow, and T_C (at low-T side) at $P = 0$ is marked with a dotted line. The number in parentheses gives the order of the measurement number. In (b), T_N at (high-T side) and T_C (at low-T side) at $P = 0$ are marked with the arrows.
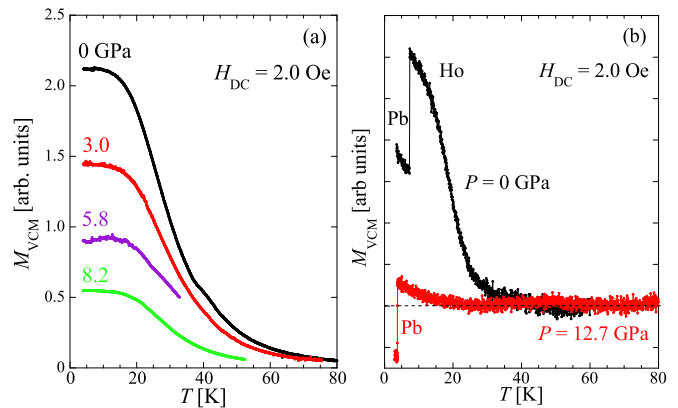

FIG. 10. T dependence of M_{VCM} in Ho, measured by method (4). M_{VCM} at the H_{DC} of 2.0 Oe was measured during the warming process after zero-field cooling over two runs [(a) the first and (b) the second run].
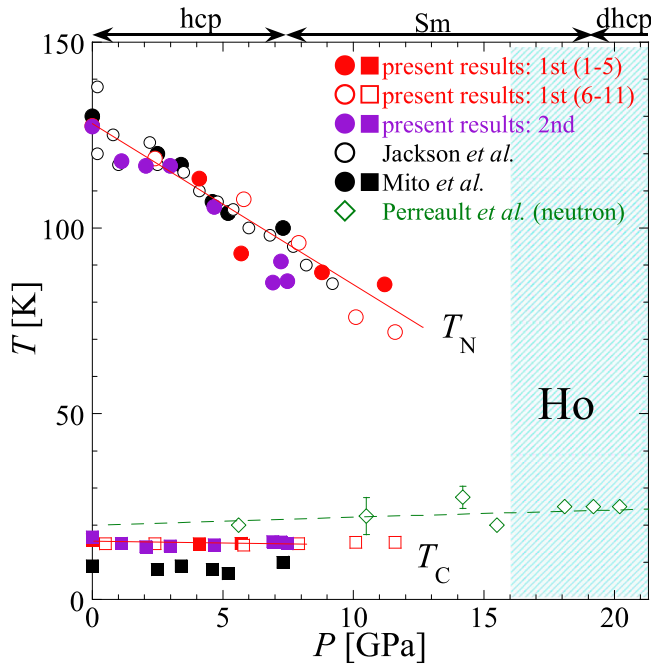
FIG. 11. P dependence of T_N and T_C in Ho. The data on T_N and T_C in the literature on magnetic measurements by Mito *et al.* [10] and Jackson *et al.* [9] are also presented. For reference, in the neutron diffraction experiment by Perreault *et al.* [18], the temperatures at which magnetic diffraction appears are also marked.

FIG. 12. The relationship between the critical pressure P_c for the disappearance of both FM and HM magnetizations and the change in the crystal structure. The pressure regions in which the FM and HM magnetizations survive are displayed with light blue and light green bars, respectively. LT and HT in parentheses stand for the low-temperature and high-temperature phases, respectively.

M_{VCM} at small H_{DC} is taken as the DC magnetic susceptibility. A superconducting lead acts as an indicator for the sign of magnetization and as a manometer at low temperatures. Method (4) has so far been used to observe the superconducting signals in an Fe-based superconductor and vanadium [30,37]. M_{VCM} at the H_{DC} of 2.0 Oe was measured during the warming process to 80 K after zero-field cooling. At $P = 0$, the increase in M_{VCM} saturates below 10 K, and this behavior does not change even at $P \neq 0$. The FM anomaly was observed at pressures of up to 8.2 GPa. The positive M_{VCM} signal against a small H_{DC} thus rules out the possibility of superconducting phenomena. Consistent with Figs. 8(a) and 9(b), the FM anomaly was not observed after transformation to the Sm-type phase [see the data for $P = 12.7$ GPa in Fig. 10(b)]. Thus, the FM magnetization disappears at 8.2–12.7 GPa.

Figure 11 shows the P dependence of T_N and T_C in Ho, together with the data from previous magnetic measurements [9,10]. The decrease in T_N with increasing P shows good consistency between the magnetic measurements by us and by Jackson *et al.* The FM signal in M_{VCM} is not a proper indicator for the determination of T_C, in contrast to M'_{AC}. The T_C determined from the M_{AC} measurements hardly changes with P, and T_C cannot be determined for $P > 8$ GPa starting from nonstrained materials. On the other hand, T_N was confirmed up to at least 12 GPa, and there was no characteristic HM signal at $P = 16.0$ GPa. This suggests that the HM signal disappears just after the crystal structure is sufficiently transformed into the Sm-type phase.
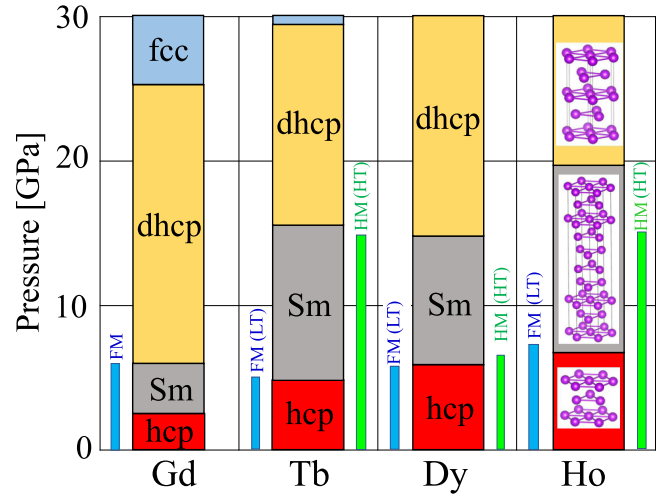
IV. DISCUSSION

A. Disappearance of magnetization along with structural change

Figure 12 shows the pressure regions in which the HM and FM magnetizations appear together with the change in the crystal structure [10]:

(1) Gd: The intensity of FM magnetization begins to decrease near the structural transformation from the hcp to Sm-type structure, and the FM magnetization disappears near the phase boundary between the Sm-type phase including the hcp domains and dhcp phases. It is experimentally known via the structural analysis that the Sm-type phase has the domains of the hcp structure. The M_{AC} intensity depends on the ratio of the FM domains with the hcp structure to the total.

(2) Tb: FM and HM magnetizations disappear near the phase boundary between the hcp and Sm-type phases and the phase boundary between the Sm-type and dhcp phases, respectively.

(3) Dy: FM and HM magnetizations disappear near the phase boundary between the hcp and Sm-type phases and slightly after entering the Sm-type phases, respectively.

(4) Ho: FM magnetization disappears at a slightly higher pressure than the phase boundary between the hcp and Sm-type phases, and the HM magnetization disappears after entering into the Sm-type phases sufficiently.

Given the aforementioned results, the FM order in Gd, Tb, Dy, and Ho can survive stably in the domains with the hcp structure. The relationship between the disappearance of the HM and FM magnetizations and the change in crystal structure is element-dependent. Information on the electronic states under pressure is important for understanding the magnetism change in Gd–Ho under pressure. However the calculation of the electronic states in $4f$ lanthanide metals is not easy, because it requires considering the spin polarization of the

localized $4f$ spins. We are attempting the density functional theory calculations for Gd with collaborators.

B. How does the neutron look at the change in stability of magnetic ordering?

For Tb, Dy, and Ho, neutron diffraction experiments have already been performed, and their results have to be considered together with the present magnetic results.

In Tb, neutron diffraction due to the FM order disappears at around the hcp-to-Sm structural transition, near which M'_{AC} due to the FM order disappears. In Tb, the disappearance of the FM order can occur at approximately 7 GPa.

In the neutron diffraction experiment for Dy by Perreaulta et $al.$, the Sm-type phase at $P = 10.8$ GPa exhibits no magnetic superlattice reflection due to the HM order. They observed an enhancement of the intensities of the nuclear peaks with decreasing temperature, so that the critical temperature was determined to be 59 K [17]. However, the intensity enhancement of the nuclear peak below 59 K is small. They concluded that there is an inhomogeneous magnetic state with FM domains coexisting within a paramagnetic state in the Sm-type phase at $P = 10.8$ GPa. As seen in Fig. 7, rather the result of "59 K at $P = 10.9$ GPa" by Perreault et $al.$ is close to the results in R by Lim et $al.$ [14,16], and it is nearly on the extrapolated line of the T_C evaluated from the M_{DC} data at $H_{DC} = 0.3$ T by Mito et $al.$ [10]. The present M'_{AC} results reveal that both HM and FM magnetizations do not survive at approximately 10 GPa. We cannot agree on the survival of the FM order in the Sm phase, but we can agree with the picture of the FM domains surviving in the paramagnetic state. We also suppose that the magnetic order for $P > P_c$ is antiferromagnetic.

In the neutron diffraction for Ho by Perreault et $al.$, the neutron diffraction detected only a commensurate superlattice formation along the c axis in both the Sm-type phase above 10 GPa and the dhcp phase above 19 GPa (see Fig. 11) [18]. Perreault et $al.$ mentioned that the FM transition marked by the appearance of a magnetic peak at 3 Å and the concurrent enhancement of nuclear peaks below 30 K [18]. However, the above phenomena are inconsistent with the results of the present magnetic measurements (M'_{AC} and M_{VCM}), which exhibit no sign of the above new FM order and definite anomaly due to the HM order at pressures up to at least 11.6 GPa. In our view, even if there is a magnetic order at approximately 20 K, it has no large net magnetic moment.

For both Dy and Ho, the magnetic peaks observed at high-pressure phases in the neutron diffraction experiments are not equivalent to the magnetic anomalies tracing the FM and HM orders observed in the present magnetic measurements at small H_{DC}. We assume that the neutron diffraction experiments for Dy and Ho above P_c would detect any magnetic order that is different from FM order stabilized at ambient pressure.

C. What does electrical resistance detect?

At $P = 0$, the electrical anomalies in R appear at the magnetic ordering temperatures, T_C in Gd [14,16], T_C in Tb (T_N and T_C are very close) [15,16], and T_N in Dy [14,16]. In the

present magnetic measurements for Tb, T_N hardly changes at the initial pressures, while T_C decreases. Consequently, the electrical change in R follows the decrease in T_C [15,16]. In the present magnetic measurements for Dy, both T_N and T_C decrease with increasing P. The electrical change in R for Dy traces the change in T_N [14,16]. Thus, in the case of multiple magnetic orderings, it depends on the element what kind of ordering the R anomaly reflects. Further, in Gd, the R anomaly can be seen after the FM magnetization disappears [14,16]. The R anomaly in Tb has been observed even after the FM magnetization disappears [15,16]. The R anomaly in Dy also survives after the HM magnetization disappears [14,16]. In Dy, the broad R anomaly at high pressures is related with the results of neutron diffraction [17] and the Mössbauer spectroscopy [19].

The RKKY interaction originates from the mediation of conduction electrons between localized magnetic moments near the nuclei. In f-electron systems, the electrical conductivity is influenced by the magnetic ordering as well as the structural transformation and the change in valence. The RKKY interaction is expressed as

$$J_{ij} = -\frac{9\pi}{4N} I_{eff}^2 D(E_F) F(2k_F |\boldsymbol{R}_i - \boldsymbol{R}_j|). \quad (1)$$

Here $\boldsymbol{R}_i$ is the lattice site of S_i, N is the total number of ions, $D(E_F)$ is the density of states at the Fermi level E_F, $F(x) = (x \cos x - \sin x)/x^4$, and k_F is the Fermi wave vector [10,38]. I_{eff} is the effective exchange integral between the conduction electrons and the localized f-orbital electrons. I_{eff} includes the mixing potential between the conduction electrons and the localized f electrons, the one-electron energy of the localized f-orbital relative to E_F, and the Coulomb repulsion between the opposite spin electrons localized on the f orbital. Generally, the lattice shrinkage under pressure lowers the bottom of the conduction band, which causes a decrease in $D(E_F)$. The decrease in J_{ij} results in a decrease in T_N and/or T_C. Furthermore, the structural phase transition can bring about a drastic change in $D(E_F)$ and I_{eff}, resulting in the disappearance of three-dimensional magnetic ordering.

Now, in Dy, we have the wealthiest information. In Sec. IV B, we have mentioned that the magnetic diffraction of "59 K at $P = 10.9$ GPa" for Dy in the neutron experiment by Perreault et $al.$ is close to the results in R by Lim et $al.$ [14,16], and it is nearly on the extrapolated line of T_C evaluated from M_{DC} at large H_{DC} by Mito et $al.$ [10]. The R anomaly may reflect any short-range ordering or small domain formation. The Mössbauer spectroscopy, however, revealed that at 10 K the hyperfine magnetic field remains almost constant with increasing pressure to 141 GPa [19]. Furthermore, x-ray absorption near edge structure reveals no change in valence at 115 GPa [19]. Thus, we cannot help recognizing that at least the R anomaly of Dy reflects the existence of magnetic order. However, it is noted that the broad R anomaly does not exhibit the nature of magnetic order. To elucidate the nature of magnetic order, theoretical calculations based on the crystal structure at high pressures will be needed.

Given this fact, the present results suggest that R for $P > P_c$ would reflect the magnetic ordering different from either FM or HM that is stabilized at ambient pressure. The RKKY interaction can change the sign and magnitude as a function of

distance between neighboring $4f$ localized moments. Indeed, M_{DC} at sufficient H_{DC} and M_{AC} at small H_{AC} do not exhibit the same anomaly shape at T_N and T_C. The present magnetic measurement does not have enough sensitivity to detect a minute signal of the antiferromagnetic ordering. In order to elucidate the magnetic order surviving at ultrahigh pressures experimentally, the spectroscopy as well as neutron diffraction experiments become more important.

V. CONCLUSION

We measured M_{AC} in Gd, Tb, Dy, and Ho using the SQUID magnetometer. For Ho, M_{VCM} was also measured. The AC measurements using SQUID have higher accuracy than DC measurements using SQUID and AC measurements by the electromagnetic induction method. The change in T_N and T_C can therefore be traced in detail and the disappearance of mag-

netization can be determined with better than in the previous measurements.

The FM magnetization in Gd, Tb, Dy, and Ho can survive within the hcp structure. The HM magnetization in Tb and Dy disappear at the Sm-to-dhcp and hcp-to-Sm structural transitions, respectively, and that of Ho disappears in the Sm-type phase near the Sm-to-dhcp structural transition.

Based on previous electrical experiments, the ordering that the R anomaly reflects depends on the element. The R anomalies for Gd, Tb, and Dy survive even after the corresponding magnetization disappears. In order to pursue the magnetic orders at high pressures in more detail, the spectroscopy experiment as well as neutron diffraction become more important.

[1] M. Ruderman and C. Kittel, Phys. Rev. **96**, 99 (1954).

[2] T. Kasuya, Prog. Theor. Phys. **16**, 45 (1956).

[3] K. Yosida, Phys. Rev. **106**, 893 (1957).

[4] J. Akella, G. S. Smith, and A. P. Jephcoat, J. Phys. Chem. Solids **49**, 573 (1988).

[5] W. A. Grosshans and W. B. Holzapfel, Phys. Rev. B **45**, 5171 (1992).

[6] W. C. Koehler and R. M. Moon, Phys. Rev. Lett. **29**, 1468 (1972).

[7] D. McWhan and A. Stevens, Phys. Rev. **139**, A682 (1965).

[8] T. Iwamoto, M. Mito, M. Hitaka, T. Kawae, and K. Takeda, Physica B **329–333**, 667 (2003).

[9] D. D. Jackson, V. Malba, S. T. Weir, P. A. Baker, and Y. K. Vohra, Phys. Rev. B **71**, 184416 (2005).

[10] M. Mito, K. Matsumoto, Y. Komorida, H. Deguchi, S. Takagi, T. Tajiri, T. Iwamoto, T. Kawae, M. Tokita, and K. Takeda, J. Phys. Chem. Solids **70**, 1290 (2009).

[11] G. K. Samudrala, G. M. Tsoi, S. T. Weir, and Y. K. Vohra, High Press. Res. **34**, 385 (2014).

[12] S. A. Thomas, J. M. Montgommery, G. M. Tsoi, Y. K. Vohra, G. N. Chesnut, S. T. Weir, C. A. Tulk, and A. M. dos Santos, High Press. Res. **33**, 555 (2013).

[13] G. K. Samudrala, G. M. Tsoi, S. T. Weir, and Y. K. Vohra, High Press. Res. **34**, 266 (2014).

[14] J. Lim, G. Fabbris, D. Haskel, and J. S. Schilling, Phys. Rev. B **91**, 045116 (2015).

[15] J. Lim, G. Fabbris, D. Haskel, and J. S. Schilling, Phys. Rev. B **91**, 174428 (2015).

[16] J. Lim, G. Fabbris, D. Haskel, and J. S. Schilling, J. Phys. Conf. Ser. **950**, 042025 (2017).

[17] C. Perreault, Y. Vohra, A. dos Santos, J. Molaison, and R. Boehler, High Press. Res. **39**, 588 (2019).

[18] C. Perreault, Y. Vohra, A. dos Santos, and J. Molaison, J. Magn. Magn. Mater. **507**, 166843 (2020).

[19] W. Bi, E. Alp, J. Song, Y. Deng, J. Zhao, M. Hu, D. Haskel, and J. M. Schilling, APS March Meeting 2017, http://meetings.aps.org/link/BAPS.2017.MAR.B35.15.

[20] M. Mito, M. Hitaka, T. Kawae, K. Takeda, T. Kitai, and N. Toyoshima, Jpn. J. Appl. Phys. **40**, 6641 (2001).

[21] M. Ishizuka, K. Amaya, and S. Endo, Rev. Sci. Instrum. **66**, 3307 (1995).

[22] M. Mito, Y. Komorida, H. Tsuruda, J. Tse, S. Desgreniers, Y. Ohishi, A. Leitch, K. Cvrkalj, C. Robertson, and R. Oakley, J. Am. Chem. Soc. **131**, 16012 (2009).

[23] A. Leitch, K. Lekin, S. Winter, L. Downie, H. Tsuruda, J. Tse, M. Mito, S. Desgreniers, P. Dube, S. Zhang *et al.*, J. Am. Chem. Soc. **133**, 6051 (2011).

[24] H. Tsuruda, M. Mito, H. Deguchi, S. Takagi, A. Leitch, K. Lekin, S. Winter, and R. Oakley, Polyhedron **30**, 2997 (2011).

[25] S. Yamaguchi, N. Yamaguchi, M. Mito, H. Deguchi, P. J. Baker, S. J. Blundell, M. J. Pitcher, D. R. Parker, and S. J. Clarke, J. Korean Phys. Soc. **63**, 445 (2013).

[26] M. Mito, T. Imakyurei, H. Deguchi, K. Matsumoto, H. Hara, T. Ozaki, H. Takeya, and Y. Takano, J. Phys. Soc. Jpn. **83**, 023705 (2014).

[27] M. Mito, H. Matsui, H. Goto, H. Deguchi, K. Matsumoto, H. Hara, T. Ozaki, H. Takeya, and Y. Takano, J. Phys. Soc. Jpn. **85**, 024711 (2016).

[28] M. Mito, K. Ogata, H. Goto, K. Tsuruta, K. Nakamura, H. Deguchi, T. Horide, K. Matsumoto, T. Tajiri, H. Hara *et al.*, Phys. Rev. B **95**, 064503 (2017).

[29] M. Mito, Y. Kitamura, T. Tajiri, K. Nakamura, R. Shiraishi, K. Ogata, H. Deguchi, T. Yamaguchi, N. Takeshita, T. Nishizaki *et al.*, J. Appl. Phys. **125**, 125901 (2019).

[30] M. Mito, S. Shigeoka, H. Kondo, N. Noumi, Y. Kitamura, K. Irie, K. Nakamura, S. Takagi, H. Deguchi, T. Tajiri *et al.*, Mater. Trans. **60**, 1472 (2019).

[31] See Supplemental Material at http://link.aps.org/supplemental/10.1103/PhysRevB.103.024444 for background data on M'_{AC} for Gd, Tb, and Ho.

[32] M. Mito, J. Phys. Soc. Jpn. Suppl. A **76**, 182 (2007).

[33] G. J. Piermarini, S. Block, J. D. Barnett, and R. A. Forman, J. Appl. Phys. **46**, 2774 (1975).

[34] J. Yamada, K. Irie, M. Mito, H. Deguchi, and S. Takagi, J. Magn. Magn. Mater. **310**, 2734 (2007).

[35] K. Irie, K. Shibayama, M. Mito, S. Takagi, M. Ishizuka, K. Lekin, and R. T. Oakley, Phys. Rev. B **99**, 014417 (2019).

[36] M. Ishizuka, Rev. Sci. Instrum. **76**, 123902 (2005).

[37] M. Abdel-Hafiez, M. Mito, K. Shibayama, S. Takagi, M. Ishizuka, A. N. Vasiliev, C. Krellner, and H. K. Mao, Phys. Rev. B **98**, 094504 (2018).

[38] M. Tokita, K. Zenmyo, H. Kubo, K. Takeda, M. Mito, and T. Iwamoto, J. Magn. Magn. Mater. **272–276**, 593 (2004).